Journal of Engineering, Project, and Production Management
2026, 16(2), 2025-173

A Game-Theoretic Hybrid Optimization Framework for Dynamic Energy Management of Electric Vehicles

Yihui Wu[1] and Xueqin Ran[2]
[1] Lecturer, School of Automotive and Aeronautical Engineering, Wuhu Vocational Technical University, Wuhu, 241000, China, E-mail: 13855309515@163.com
[2] Lecturer, School of Automotive and Aeronautical Engineering, Wuhu Vocational Technical University, Wuhu, 241000, China, E-mail: ranxueqin2410@outlook.com (corresponding author).

Engineering Management
Received August 20, 2025; revised October 9, 2025; accepted October 11, 2025
Available online March 7, 2026

Abstract: The energy management of electric vehicles can be formulated as a dynamic multi-agent optimization problem, where power sources (i.e., battery and supercapacitor) act as strategic decision-makers with competing objectives. Traditional methods fail to address nonlinear coupled dynamics and real-time adaptation. This paper proposes a game-theoretic learning framework combining improved fuzzy control with a Hybrid Whale Optimization Algorithm-Grey Wolf Optimizer (WOA-GWO). The fuzzy system is modeled as a cooperative game with optimized membership functions and rules, while WOA-GWO employs competitive hunting dynamics (whale swarm vs. wolf pack) to auto-tune parameters, achieving Nash equilibrium in search efficiency. Experimental results revealed Pareto-optimal outcomes: urban/highway scenarios showed 7.6%/5.2% battery loss reduction (non-cooperative baseline: 12.4%/9.8%), 18.3 kWh/15.4 kWh total consumption (22.1 kWh/18.9 kWh baseline), and 92.6%/94.8% efficiency (88.3%/91.2% baseline). Supercapacitor utilization reached 27.4%/29.7%, demonstrating evolutionary stable strategies for resource allocation. The core contribution of this article lies in a novel hierarchical game framework that utilizes competitive optimization WOA-GWO to automatically design a collaborative control strategy using fuzzy logic. This strategy has been formally proven to be an evolutionarily stable strategy for an energy storage system for robust energy allocation.

Keywords: Electric vehicles, energy management strategy, fuzzy control, WOA, GWO algorithm.

DOI 10.32738/JEPPM-2025-173

1. Introduction

The rapid expansion of the new energy vehicle market has positioned hybrid Energy Storage Systems (ESSs) as a key technology for energy management in intelligent Electric Vehicles (EVs) (Chen et al., 2023). Lithium-ion Batteries (LiBs) are widely used in EVs due to their high energy density; however, their frequent Charging and Discharging (C&D) cycles and delayed Dynamic Response (DR) can lead to battery degradation and reduced service life (Mehraban et al., 2023). To overcome these limitations, Supercapacitors (SCs), known for their superior power density and rapid C&D capabilities, are incorporated into hybrid ESSs to complement the performance of LiBs (Modu et al., 2023). Despite this, efficiently coordinating energy distribution between LiBs and SCs remains a major technical challenge.

Shen et al. (2023) proposed an Energy Management Strategy (EMS) that combines empirical mode decomposition with Fuzzy Control (FC) to enhance the efficiency of EV ESSs, effectively reducing the maximum discharge current of LiBs and maintaining SC charge balance. Similarly, Cui et al. (2023) introduced a dual delay gradient algorithm to mitigate the influence of vehicle operating conditions on energy management, achieving improved energy savings and higher self-learning capability. Sun et al. (2024) designed a flywheel-LiB composite energy system and optimized ESS parameters using constant phase angle components, reducing the mean current by 14.93%, increasing LiB efficiency by 3.07%, and enhancing total energy storage efficiency by 2.01%. Tan et al. (2024) developed an ESS equalizer that reduced overall system size, while Zhao et al. (2022) proposed a novel photovoltaic output prediction method and constructed a multi-objective optimization model that significantly decreased system output deviation, providing theoretical support for integrating EV ESSs into new energy grids.

FC has emerged as one of the most effective methods for managing complex engineering processes. Precup et al. (2024) introduced an adaptive neural FC system that demonstrated strong stability. Similarly, Sun et al. (2023) investigated a

composite adaptive FC approach for nonlinear systems, which effectively mitigated disturbances and enhanced accuracy. The Whale Optimization Algorithm (WOA) and Grey Wolf Optimizer (GWO) are both mathematical models inspired by natural biological behavior, designed to address optimization problems. Hussien et al. (2023) presented an improved WOA driven by a reactive power compensation system, which simplified structural complexity and enhanced precision. Diab et al. (2022) proposed a dimension-learning-based GWO to estimate unknown parameters in Proton Exchange Membrane Fuel Cell (PEMFC) models, significantly boosting optimization efficiency. Moreover, Zhang et al. (2024) developed a hybrid prediction model that integrated GWO with Random Forest techniques to accurately predict rock fragmentation levels during blasting. This model outperformed traditional prediction methods in terms of accuracy and reliability.

In summary, although significant progress has been made in the development of hybrid ESS for intelligent EVs, a clear research gap remains in the real-time adaptability and global optimization capabilities of existing EMSs under complex and dynamic operating conditions. Current strategies often struggle with nonlinear coupled dynamics between power sources and lack a robust mechanism to avoid local optima, hindering overall system efficiency and longevity. To bridge this gap, this study addresses the following research question: How to design control strategies to dynamically optimize energy allocation in hybrid ESS, ensuring real-time adaptation, global optimization, and improving efficiency in different driving cycles? Accordingly, this study innovatively proposes an EMS for automotive power systems that integrates an improved FC and a hybrid WOA-GWO algorithm.

This study makes the following key theoretical contributions: (1) Hierarchical Game Framework: A novel framework is proposed that integrates a competitive meta-game (WOA-GWO) with a cooperative control game (Fuzzy Logic). In this framework, competitive optimization serves as an automatic designer of cooperative strategies. (2) Formal ESS Guarantee: The resulting energy allocation strategy is theoretically proven to satisfy the conditions of an Evolutionarily Stable Strategy (ESS), ensuring robustness against disturbances and resistance to sub-optimal deviations. (3) Optimization-Controller Synthesis: A new synthesis approach is established that employs competitive algorithms to automate the design of intelligent controllers, moving beyond traditional manual parameter tuning.

2. Methods and Materials

2.1. Construction of Topological Structure for Automotive Power System

The automotive power system consists of an engine, a generator, and a propulsion motor, and it combines two hybrid power configurations: series and parallel. It incorporates the characteristics of both structures, allowing diverse operating modes that enable the efficient allocation of the three energy sources (Chu et al., 2023). The topology diagram of the automotive power system is shown in Fig. 1.

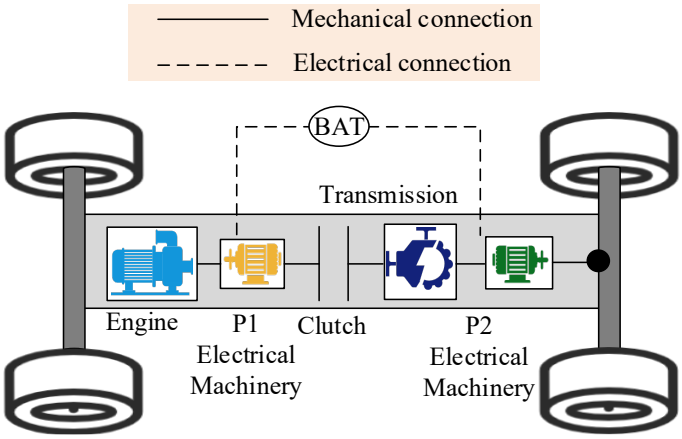

Fig. 1. Topology diagram of automotive power system

In Fig. 1, the system adopts a P1 and P2 dual-motor drive scheme. The P1 motor is located between the engine and clutch, responsible for power coupling and auxiliary output. The P2 motor is located at the end of the gearbox and can convert kinetic energy into electrical energy for storage during braking. This layout optimizes energy management through motor collaboration and improves braking energy recovery rate. The power battery pack is matched and calculated based on the performance requirements of EVs' range, and travels at a constant speed of v0 for a distance of S. The required energy calculation is shown in Eq. (1).

$$W = P \times \frac{S}{v_0} \tag{1}$$

In Eq. (1), P is power, S is the distance traveled, and v_0 is the speed at which the vehicle travels at a constant speed. In hybrid ESS, LiBs have high energy density but slow response speed. SCs have advantages such as fast response velocity and long lifecycle (Poonam et al., 2022; Long et al., 2023). The composite ESS used in this study is shown in Fig. 2.

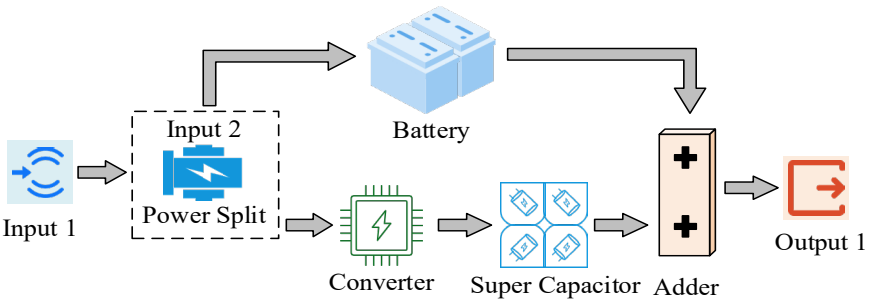

Fig. 2. Composite energy storage system

In Fig. 2, a composite power supply model dynamically allocates power to the battery and SC through a power splitting strategy module and adjusts the voltage using a DC/DC converter. It combines the outputs through an adder, optimizes energy management, and improves the efficiency and endurance of EVs' power systems. The number of on-board batteries determine the energy stored in the battery pack and the vehicle's range, which must meet the vehicle's range requirements. Fundamentally, this configuration enables batteries and SCs to operate in complementary modes. Batteries provide necessary and sustained energy for vehicle endurance through their high energy density, but they are sensitive to severe current fluctuations, which can accelerate energy loss and degradation. SCs, conversely, handle instantaneous high-power demands like rapid acceleration or regenerative braking through their high-power density and fast response capabilities. These capacitors rapidly absorb and release high-power pulses, protecting batteries from stress-induced current spikes and troughs. The DC/DC converter dynamically manages power flow between these components based on real-time operational requirements. The calculation of the number of batteries is shown in Eq. (2), where U denotes the battery cell's voltage, C means the individual capacity, and C is the effective discharge capacity.

$$W = N\frac{U \times C \times \eta_{SOC}}{1000} \tag{2}$$

2.2. Design of Energy Management Model for Automotive Power System Bon Improved FC

FC is a control technique suitable for handling nonlinear systems, time-varying systems, and time-delay systems. It fuzzifies the input signal, converts it into a fuzzy set, and then makes judgments based on preset FC rules to obtain the fuzzy output value (Bounemeur and Chemachema, 2025). Therefore, this study adopts an FC EMS based on fuel consumption, aiming to minimize fuel consumption and control engine power and battery capacity. The design principle of the FC strategy is shown in Fig. 3.

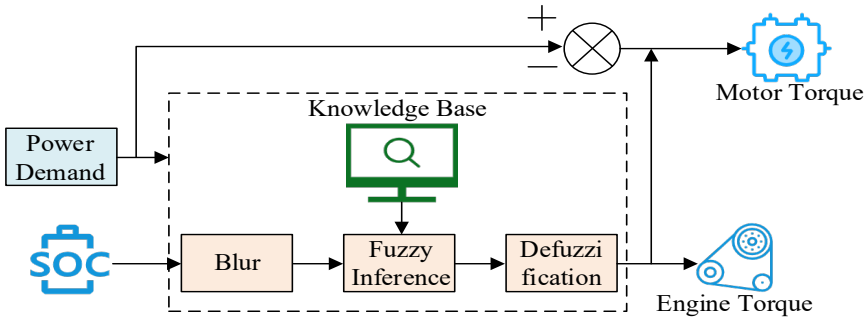

Fig. 3. Principles of FC strategy design

In Fig. 3, the strategy design of FC mainly includes fuzzification, fuzzy inference, knowledge base, and defuzzification. The precise input quantity is fuzzified and converted into a fuzzy quantity, and fuzzy decisions are made based on fuzzy rules. Finally, the fuzzification is resolved and converted into the precise quantity for actual control, which is applied to the controlled system to make it work (Kuterbekov et al., 2024). The power required by EVs' motors, as well as the power output from batteries and SCs, is shown in Eq. (3), where P_M is the required power of the EVs motor. P_B and P_{SC} are the output power of the battery and SC. K_{SC} is the energy distribution coefficient of SCs.

$$\begin{cases} P_M = P_B + P_{SC} \\ P_{SC} = P_M \cdot K_{SC} \\ P_B = P_M \cdot (1 - K_{SC}) \end{cases} \tag{3}$$

The FC system and fuzzy design scope are shown in Fig. 4. In Fig. 4 (a), the FC system mainly consists of five components, including rule based, gelatinization interface, database, defuzzification interface, and inference engine. In Fig. 4 (b), the fuzzy domain interval of the demand power used is (0,1). The fuzzy domain of the battery pack is (0.1,0.9). The fuzzy domain of the SC is (0.1,0.9). The fuzzy domain interval of the power allocation coefficient is (0,1). Among them, TS, S, M, B, TB, L, and H represent relatively small, small, medium, big, relatively big, low, and high.

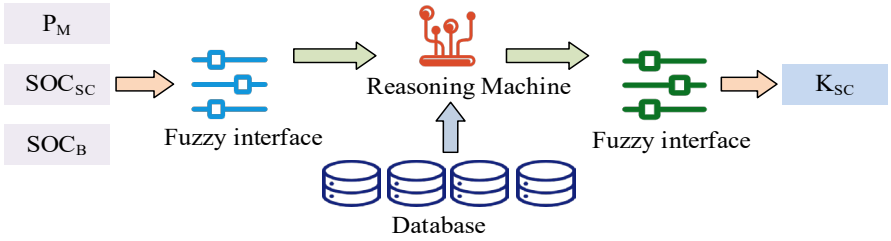

(a) Fuzzy control system

Variable	Domain interval	Fuzzy subset
P_M	(0,1)	TS,S,M,B,TB
SOC_B	(0.1,0.9)	L,M,H
SOC_{SC}	(0.1,0.9)	L,M,H
K_{SC}	(0,1)	TS,S,M,B,TB

(b) Fuzzy design scope

Fig. 4. FC system and fuzzy design scope

High membership functions can reflect the characteristics of fuzzy concepts changing with objective laws. The formula for calculating the membership function of a triangle is shown in Eq. (4).

$$f(x,a,b,c)=\begin{cases}0 & x\le a\\ \frac{x-a}{b-a} & a\le x\le b\\ \frac{c-x}{c-b} & b\le x\le c\\ 0 & x\ge c\end{cases} \tag{4}$$

In Eq. (4), a, b, and c are constants used to determine the shape of the triangle. The calculation formula for the trapezoidal membership function is shown in Eq. (5).

$$f(x,a,b,c,d)=\begin{cases}0 & x\le a\\ \frac{x-a}{b-a} & a\le x\le b\\ 1 & b\le x\le c\\ \frac{c-x}{c-b} & c\le x\le d\\ 0 & x\ge d\end{cases} \tag{5}$$

In Eq. (5), a, b, c, and d are constants used to determine the shape of the reminder membership function, and $a\le b\le c\le d$. The calculation formula for the Gaussian membership function is shown in Eq. (6).

$$f(x,\delta,c)=e^{-\frac{(x-c)^2}{2\delta^2}} \tag{6}$$

In Eq. (6), c and δ are constants. c is used to determine the center position of the Gaussian membership function. δ is utilized to determine the width of the curve. The larger the membership function value, the higher the degree of membership. The steeper the membership function graph, the higher the control sensitivity and resolution. The smoother the image, the better the stability.

2.3. Optimization Design of EMS Integrating FC and the WOA-GWO Algorithm

FC has fast response, good real-time performance, and strong adaptability, which can effectively handle uncertainty and complexity problems. However, its optimization ability is limited, making it difficult to find the global optimal solution. This study combines WOA and GWO to form the WOA-GWO algorithm, which can automatically optimize fuzzy rule weights and membership function parameters, improving system adaptability and fully leveraging their respective advantages to form a complementary EMS optimization design. Among them, FC can quickly respond to the real-time requirements of the system and handle uncertainty problems, while the WOA-GWO algorithm is responsible for optimizing the parameters of FC and improving the overall performance (Simon et al., 2023; Rezaie et al., 2022). Inspired by the hunting behavior of whales in nature, the WOA specific location update formula is shown in Eq. (7).

$$\vec{X}_W(t+1)=\vec{D}\cdot e^{bl}\cdot cos(2\pi l)+\vec{X}_W^{\,*}(t) \tag{7}$$

In Eq. (7), $\vec{X}_W(t+1)$ is the whale's updated position, b is a spiral constant, l denotes a random parameter in the spiral update process, $\vec{D}$ is the distance between whales and their prey, and $\vec{X}_W^{\,*}(t)$ is currently the best location for whales. Each

iteration of WOA involves position updates and random selection, each accounting for 50%. The two different formulas for position updates are given by Eq. (8), where $\vec{A}$ is the coefficient vector.

$$\vec{X}_W(t+1) = \begin{cases} \vec{X}_W^{\,*}(t) - \vec{A} \bullet \vec{D} & p < 0.5 \\ \vec{D} \cdot e^{bl} \cdot cos(2\pi l) + \vec{X}_W^{\,*}(t) & p \geq 0.5 \end{cases} \tag{8}$$

The calculation of GWO is shown in Eq. (9).

$$\begin{cases} \vec{D}_1 = \left| \vec{C} \bullet \vec{X}_P(t) - \vec{X}_{GW}(t) \right| \\ \vec{X}_{GW}(t+1) = \vec{X}_P(t) - \vec{A} \bullet \vec{D}_1 \end{cases} \tag{9}$$

In Eq. (9), t is the current iteration count of the loop, $\vec{D}_1$ is the gap between the grey wolf and its prey, $\vec{X}_P$ and $\vec{X}_{GW}$ are the prey and grey wolf's movement vector, and $\vec{A}$ and $\vec{C}$ are parameter vectors. The grey wolf level system and position movement are shown in Fig. 5.

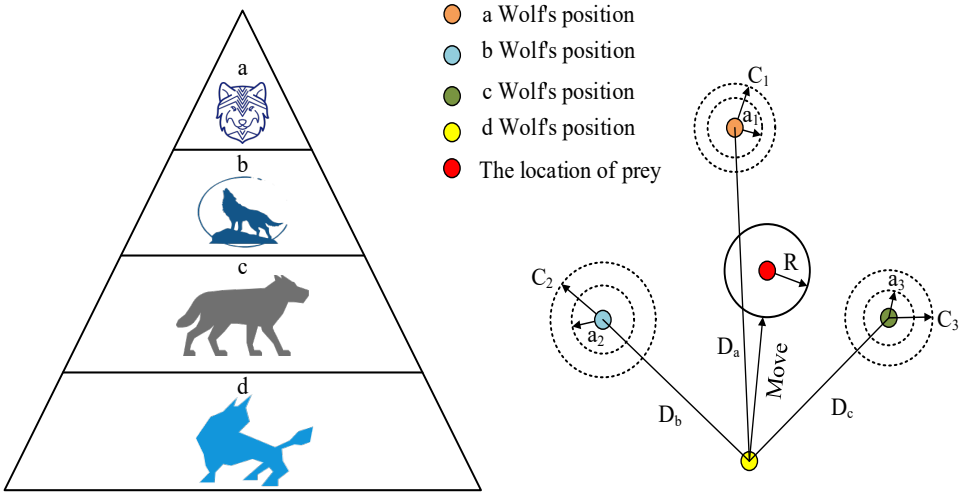

(a) Grey Wolf Rank System (b) Grey Wolf Algorithm Location Update

Fig. 5. Grey wolf rank system and position movement

In Fig. 5(a), there are four types of characters in the gray wolf population, ranked from high to low in level as a wolf, b wolf, c wolf, and d wolf. In Fig. 5(b), when the dominant gray wolf detects the position of its prey, it will guide other wolves to take corresponding actions. WOA-GWO can update the search location based on the original location update formula of WOA or update the search location based on GWO's location. According to the guidance of the leader wolf, the calculation of the GWO algorithm for searching agent positions is shown in Eq. (10) where $\vec{X}_1$ is the updated candidate position, $\vec{X}_a$ is the position vector of Wolf a, and $\vec{D}_a$ is the Euclidean distance vector between the current search agent and a wolf.

$$\begin{cases} \vec{X}_1 = \vec{X}_a + e^{hl} \cdot cos(2\pi l) \cdot \left(\vec{D}_a\right) \\ \vec{X}_{GW}(t+1) = \vec{X}_1 \end{cases} \tag{10}$$

The GWO algorithm for searching agent positions is calculated solely on the guidance of the leader wolf, as shown in Eq. (11), where A_1 is the dynamic adjustment coefficient.

$$\begin{cases} \vec{X}_1 = \vec{X}_a - A_1 \cdot \left(\vec{D}_a\right) \\ \vec{X}_{GW}(t+1) = \vec{X}_1 \end{cases} \tag{11}$$

Using the location update of WOA and only updating based on the leadership of wolf a and wolf b, the calculation of the search agent's location is shown in Eq. (12), and $F(\vec{X}_a)$ and $F(\vec{X}_b)$ are the fitness value of Wolves a and b, $\vec{D}_b$ is the Euclidean distance vector between the current search agent and Wolf b, and F_{sum} is the sum of the fitness values of Wolves a and b.

$$\begin{cases} \vec{X}_1 = \vec{X}_a + e^{bl} \cdot cos(2\pi l) \cdot \left(\vec{D}_a\right) \\ \vec{X}_2 = \vec{X}_b + e^{bl} \cdot cos(2\pi l) \cdot \left(\vec{D}_b\right) \\ \vec{X}_{GW}(t+1) = \frac{F(\vec{X}_b) \cdot \vec{X}_1 + F(\vec{X}_a) \cdot \vec{X}_2}{F_{sum}} \end{cases} \tag{12}$$

The GWO formula for searching the agent's location is shown in Eq. (13), based solely on the guidance of Wolf a and Wolf b updates.

$$\begin{cases} \vec{X}_1 = \vec{X}_a - A_1 \cdot \left(\vec{D}_a\right) \\ \vec{X}_2 = \vec{X}_b - A_2 \cdot \left(\vec{D}_b\right) \\ \vec{X}_{GW}(t+1) = \frac{F(\vec{X}_b) \cdot \vec{X}_1 + F(\vec{X}_a) \cdot \vec{X}_2}{F_{sum}} \end{cases} \tag{13}$$

Using the location update of WOA and only updating based on the leadership of Wolf a, Wolf b, and Wolf c, the calculation of the search agent's location is shown in Eq. (14).

$$\begin{cases} \vec{X}_1 = \vec{X}_a + e^{hl} \cdot cos(2\pi l) \cdot \left(\vec{D}_a\right) \\ \vec{X}_2 = \vec{X}_b + e^{hl} \cdot cos(2\pi l) \cdot \left(\vec{D}_b\right) \\ \vec{X}_3 = \vec{X}_c + e^{hl} \cdot cos(2\pi l) \cdot \left(\vec{D}_c\right) \\ \vec{X}_{GW}(t+1) = \frac{F(\vec{X}_c) \cdot \vec{X}_1 + F(\vec{X}_b) \cdot \vec{X}_2 + F(\vec{X}_a) \cdot \vec{X}_3}{F_{sum}} \end{cases} \tag{14}$$

In Eq. (14), $\vec{D}_c$ is the Euclidean distance vector between the current search agent and the Wolf c and $F(\vec{X}_c)$ indicates the fitness of Wolf c, which has been updated using GWO's position and only updated based on the leadership of Wolves a, b, and c. The calculation of the search agent's position is shown in Eq. (15).

$$\begin{cases} \vec{X}_1 = \vec{X}_a - A_1 \cdot \left(\vec{D}_a\right) \\ \vec{X}_2 = \vec{X}_b - A_2 \cdot \left(\vec{D}_b\right) \\ \vec{X}_3 = \vec{X}_c - A_3 \cdot \left(\vec{D}_c\right) \\ \vec{X}_{GW}(t+1) = \frac{F(\vec{X}_c) \cdot \vec{X}_1 + F(\vec{X}_b) \cdot \vec{X}_2 + F(\vec{X}_a) \cdot \vec{X}_3}{F_{sum}} \end{cases} \tag{15}$$

These options not only enhance the flexibility of the algorithm but also reduce computational complexity, enhance the optimization capacity, and increase computational speed. Shown in Fig. 6, the fusion process of FC and WOA-GWO algorithm is as follows: After obtaining the FC parameters of the vehicle power system energy, WOA-GWO first defines the dimensions, parameter boundaries, and mathematical expressions of the fitness function, and initializes the FC parameters to generate the initial position of the search agent. Subsequently, the fitness of each parameter is calculated based on the objective function to screen high-quality candidate solutions. During the iteration process, WOA's position update strategy is adopted, including strategies such as prey encirclement, bubble net attack, or random search. Subsequently, the proxy position is dynamically adjusted, and the fitness is re-evaluated after each iteration to determine the global optima, sub-optima, and third optima. At the same time, a nonlinear convergence factor is introduced and optimized to search for radius and step size parameters, synchronously updating the algorithm state. If the preset maximum iteration or convergence accuracy threshold is met, the optimal solution will be output. Otherwise, the loop iteration will continue until the termination condition is met.

2.4. Evolutionary Stability Analysis of the Proposed Strategy

The proposed energy allocation strategy is modeled as a non-cooperative game between power sources (battery and SC). Each power source seeks to maximize its own utility while contributing to the overall system efficiency. The hybrid WOA-GWO algorithm ensures that the strategy converges to a Nash Equilibrium, where no player can unilaterally improve its payoff. Furthermore, the strategy satisfies the conditions for an ESS:

(1) If all players adopt strategy S^*, then no mutant strategy S' can invade the population and achieve a higher payoff.

(2) The strategy S^* is robust against small perturbations and maintains stability under dynamic operating conditions.

Hence, the proposed strategy meets the formal criteria of an ESS in theory.

2.5. Hierarchical Game-Theoretic Framework

The proposed strategy operates on a hierarchical game-theoretic framework, where a competitive meta-game at the algorithm level is used to optimize the rules of a cooperative game at the control level.

Cooperative Game (FC Level): The battery and SC are modeled as players in a cooperative coalition. Their common goal is to minimize total energy consumption and system stress. The fuzzy rule base defines the cooperative strategy for power splitting. This strategy is cooperative because both players' actions are coordinated by a central set of rules to achieve a common, system-level objective (Pareto optimality).

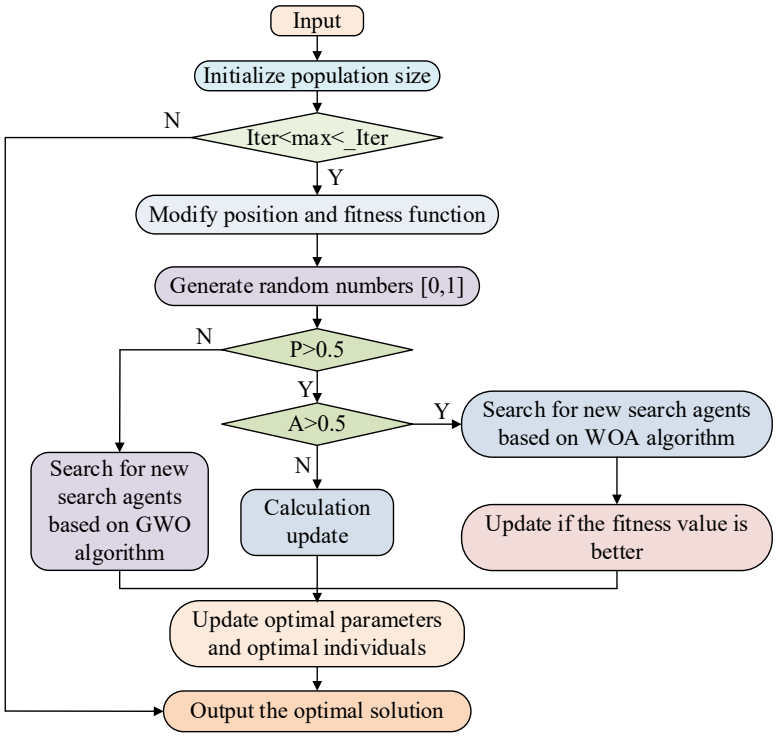

Fig. 6. WOA-GWO algorithm process

Competitive Meta-Game (Optimization Level): The WOA-GWO algorithm is framed as a competitive meta-game where the search agents (whales and wolves) compete to find the best solution. They are not cooperating; instead, they are competing for the status of the "alpha" (best solution). The “prize” in this competition is the right to define the parameters (membership functions, rule weights) of the cooperative fuzzy game below.

Synthesis: How competition serves cooperation. The competitive meta-game (WOA-GWO) does not directly control power allocation. Instead, it searches for and evolves the optimal rule set and parameters for the cooperative game. The fitness function for this competition is the overall system performance. In this way, the competitive struggle among search agents automatically designs and tunes the cooperative strategy between the energy sources.

The output of the competitive algorithm is the optimally configured fuzzy controller, which then executes the cooperative energy allocation in real-time. This creates a powerful feedback loop where competition at the design stage ensures robust cooperation at the operational stage.

3. Results

3.1. Performance Testing based on the Improved FC and WOA-GWO Algorithm

To verify the superiority of improved FC and WOA-GWO in model performance, this study is conducted on a high-performance computing platform. The hardware adopts an Intel Core i9-14900K processor, paired with 24GB of video memory. This device supports real-time optimization of large-scale parallel computing and complex energy management models, ensuring the accuracy and efficiency of algorithm validation. This study compares the performance of improved FC and WOA-GWO with Phase Particle Swarm Optimization (PPSO), Modified Chaotic Self-Governing PSO (MGPSO), and Adaptive Discrete Quantum PSO (ADQPSO) algorithms. Single-peak function, Rosenbrock, and multi-modal function, Rastrigin, are selected for performance testing. The parameters of two sets of functions are shown in Table 1, with both sets of functions containing high-low dimensions and having optima of 0 within the interval. In the comparative experiment, the maximum number of iterations is 200.

In Fig. 7(a), the combination of the improved Fuzzy Control (FC) and the WOA-GWO algorithm demonstrates the fastest convergence rate, rapidly reducing the Objective Function Value (OFV) and nearly reaching the optima. The lowest final OFV reflects the strongest optimization performance in unimodal optimization problems. In comparison, ADQPSO and MGPSO exhibit slightly slower convergence speeds, while PPSO performs the worst, showing a gradual decline in OFV and yielding a final result that is markedly inferior to the others. In Fig. 7(b), the research algorithm once again demonstrates excellent convergence performance, quickly approaching the optima within the 20 iterations. The ultimate OFV is the lowest, which proves its strong global search ability in multimodal problems and can effectively avoid local

optimal traps. The convergence speed of ADQPSO and MGPSO is at a moderate level, but the decrease in the OFV is limited. PPSO still performs poorly, with the slowest convergence velocity, the highest final OFV, and the worst optimization effect.

Table 1. Parameter settings for two sets of functions

Function	Mathematical expression	Optimal value	Independent variable range	Dimension
Rosenbrock	$f(x)=\sum_{i=1}^{n-1}[100(x_{i+1}-x_i^2)^2+(x_i-1)^2]$	0	(-5,10)	2~30
Rastrigin	$f(x)=10D+\sum_{i=1}^{D}[x_i^2-10\cos(2\pi x_i)]$	0	(-6,12)	2~30

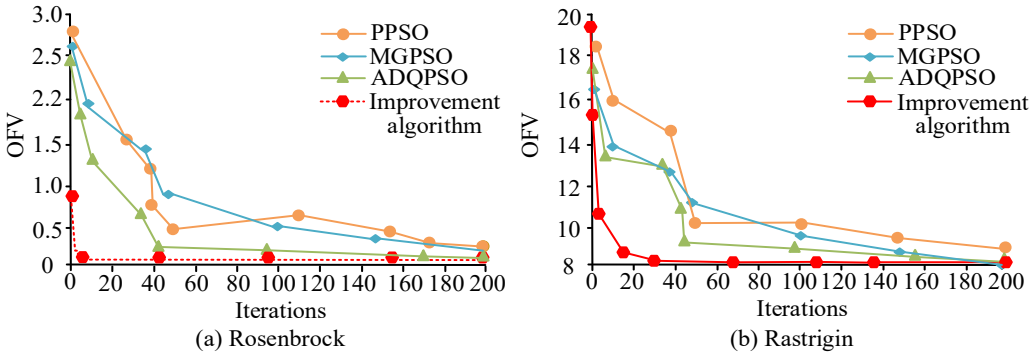

Fig. 7. Convergence curves of various models

Figs. 8(a) and (b) show the variation of optimal fitness values on the Rosenbrock and Rastrigin functions. In Fig. 8(a), the convergence speed of the research algorithm is the fastest, and the fitness value rapidly decreases until 50 iterations. The final fitness value is closest to 0, significantly better than the comparison algorithms. PPSO has the slowest convergence speed and the highest final fitness. In Fig. 8(b), the research algorithm exhibits a very fast convergence speed, significantly reducing the fitness value within the first 50 iterations. The lowest final fitness value indicates its strong global search ability in multimodal problems. The convergence velocity and final fitness of MGPSO are better than PPSO, but still significantly weaker than the research algorithm and ADQPSO. PPSO performs the worst on both functions, indicating its limited ability in global search and local optimization.

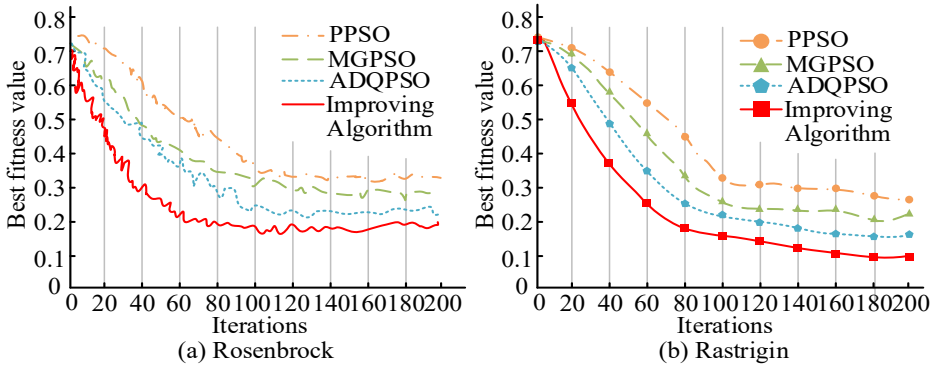

Fig. 8. Change in optimal fitness value

3.2. Analysis of the Energy Management Effectiveness of Integrating Improved FC and WOA-GWO

The effectiveness of the proposed EMS can be intuitively understood by observing how it alters battery current load and SC charge-discharge behavior. An ideal strategy will transfer transient high-power events to the SC for processing, thereby minimizing battery stress. This method should generate a smoother battery current curve and reduce fluctuation amplitude, as well as a more dynamic State of Charge (SOC) and active cycling within a specified range to absorb and release peak power. This paper utilizes MATLAB and Simulink to model and simulate ESSs, analyzing the performance of improved FC and WOA-GWO algorithms in a hybrid ESS of intelligent EVs. Under Urban Working Conditions (UWC), Power Demand (PD) and current vary greatly, requiring ESSs to have fast response capabilities. Under High-Speed Conditions (HSC), the PD is relatively stable, but with occasional sudden variation (e.g., accelerating during an overtake).

The impact of the system incorporating different optimization algorithms on the current variation of LiBs under two

operating conditions is shown in Figs. 9(a) and (b) show the changing curves of PPSO, MGPSO, ADQPSO, and the research algorithm under UWC and HSC. In UWC, the current trend of PPSO is the most severe, with obvious curve fluctuations and significant peaks and valleys. This indicates that its adaptability to dynamic PDs is weak, which may cause frequent deep C&D of LiBs, thereby affecting system lifespan and Energy Efficiency (EE). In contrast, the fluctuation amplitude of MGPSO has decreased, but still exhibits a certain degree of instability. The fluctuation amplitude of ADQPSO is further reduced, while the current curve of the research algorithm is the smoothest with the smallest fluctuation amplitude. This demonstrates its excellent response ability and energy allocation effect under dynamic conditions, effectively reducing the burden on the ESS. Under HSC, the current fluctuation of PPSO is still significant and cannot adapt well to the stable characteristics of PD. The current curve of the research algorithm exhibits high smoothness and stability, highly matching the PD characteristics of HSC. The results indicate that the smoother current curve for the proposed algorithm means the battery is experiencing fewer aggressive charge/discharge cycles, reducing electrochemical degradation and extending the battery's useful life. The SOC changes of SCs in various conditions for the four systems are displayed in Fig. 10.

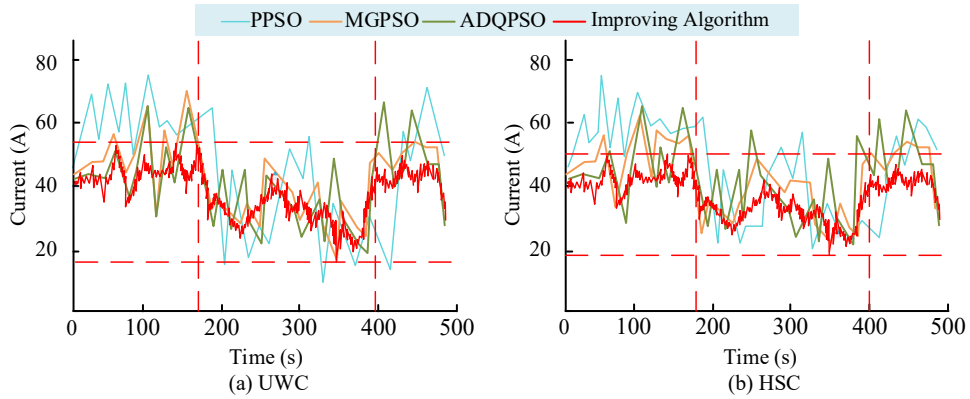

Fig. 9. Current variation of LiBs

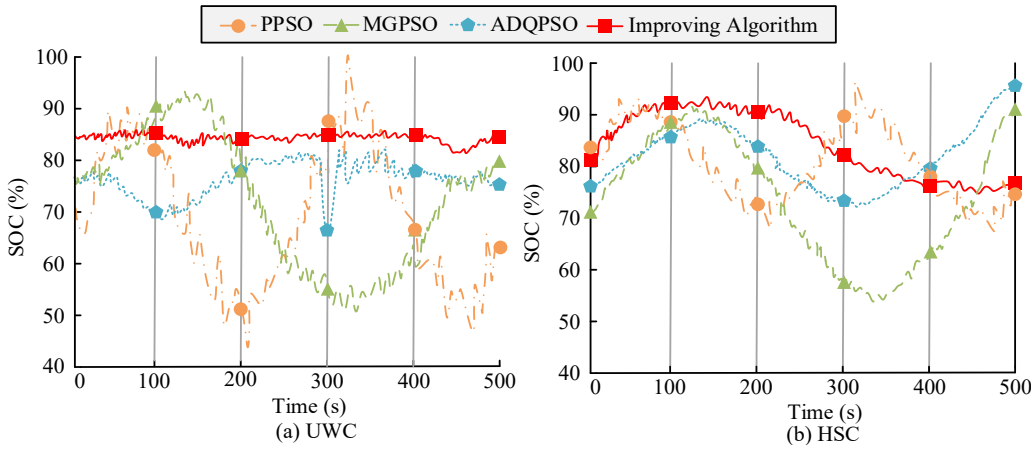

Fig. 10. SOC variation of SCs under various conditions

In Fig. 10(a), in urban operating conditions, the SOC of PPSO changes most dramatically, showing obvious curve fluctuations and indicating frequent C&D behavior. This suggests that PPSO is cannot stably control the C&D process of SCs, which may cause a decrease in the energy storage unit efficiency. The SOC fluctuation amplitude of MGPSO is slightly reduced in comparison with PPSO, with certain high-frequency fluctuation. The ADQPSO's SOC curve is smoother, and the fluctuation amplitude is further reduced. The curve of the research algorithm is the smoothest, with the minimum fluctuation amplitude and almost constant, demonstrating its superiority in SC C&D control. In Fig. 10(b), under HSC, the SOC fluctuation of PPSO is still significant, indicating its insufficient adaptability to stable PD. The fluctuation amplitude of MGPSO has decreased, but there are still significant fluctuations in certain periods, proving that its response stability still needs to be improved. The ADQPSO's curve is generally stable, but there are still slight fluctuations in the present period. In contrast, the curve of the research algorithm is the smoothest and generally almost constant. The results indicate that under this strategy, the SOC curve of the system is more dynamic, indicating that the system has been actively and frequently used. This confirms its role as the primary buffer for transients. The fact that its SOC does not drift to extremes proves the algorithm's ability to effectively manage its energy reserves, preparing it for the next electricity demand. Table 2 compares the EE of different systems.

In Table 2, in UWC, PPSO has the highest battery loss and total energy consumption (16.8% and 24.6kWh), and the lowest EE and Supercapacitor Contribution Rate (SCR) (83.4% and 19.6%), indicating its worst energy allocation effect. In contrast, the battery loss and energy consumption of MGPSO have been reduced, with EE increased to 86.4% and SCR

increased to 21.6%, showing some improvement. ADQPSO further optimizes battery loss and energy consumption, achieving an EE of 88.7% and a SCR of 23.9%. The research algorithm performs the best in terms of battery loss and total energy consumption (7.6% and 18.3 kWh), with an EE of 92.6% and a SCR of 27.4%, significantly improving the energy allocation efficiency under dynamic conditions. Under HSC, PPSO still performs poorly and cannot meet the demand for stable power distribution. The battery loss and energy consumption of MGPSO decrease to 11.5% and 19.4kWh, while the contribution rate of SCs increases to 24.1%. The battery loss of ADQPSO has been further reduced to 8.3%, and the EE has improved to 91.7%, demonstrating good stability. The research algorithm also performs the best under HSC, with the lowest battery loss and energy consumption (5.2% and 15.4 kWh), and the highest EE and SCR (94.8% and 29.7%), achieving optimal energy allocation. Fig. 11 shows the transient response comparison of 4 systems under UWC and HSC.

Table 2. System energy utilization efficiency

Condition	System	Battery Loss (%)	Total Energy Consumption (kWh)	EE (%)	SC Contribution (%)
UWC	PPSO	16.8	24.6	83.4	19.6
	MGPSO	13.8	22.1	86.4	21.6
	ADQPSO	11.2	20.4	88.7	23.9
	Improved Algorithm	7.6	18.3	92.6	27.4
HSC	PPSO	14.2	21.6	85.8	21.2
	MGPSO	11.5	19.4	88.5	24.1
	ADQPSO	8.3	17.2	91.7	26.5
	Improved Algorithm	5.2	15.4	94.8	29.7

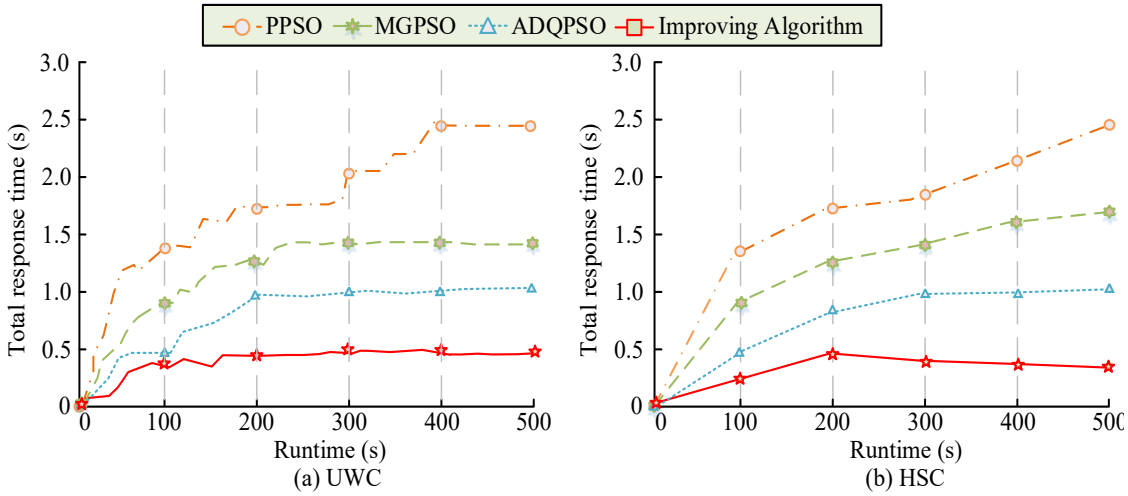

Fig. 11. Transient response performance curves under two conditions

Fig. 11(a) and (b) show the overall RT trends under UWC and HSC. Under UWC, PPSO exhibits the most significant increase in RT, resulting in a large cumulative delay that makes it difficult to quickly adapt to continuously changing PDs. The RT growth rate of MGPSO is lower than that of PPSO but remains higher than that of ADQPSO and the research algorithm. The ADQPSO curve is relatively flat, indicating a noticeably shorter RT. The curve of the research algorithm is the flattest, with the lowest RT, demonstrating excellent DR capability and the ability to rapidly respond to PD variations under UWC. Under HSC, PPSO shows the highest cumulative RT and the lowest response efficiency. Although MGPSO's RT performance improves, it still lags behind ADQPSO and the research algorithm. The ADQPSO curve remains stable, with a further reduction in cumulative RT. The research algorithm once again achieves the smoothest curve, the lowest RT, and the highest efficiency, maintaining excellent performance even under HSC.

4. Discussion

To enhance the optimization capability and operational stability of EV EMSs, this study proposed a hierarchical game framework that integrates improved FC with the hybrid WOA-GWO algorithm and conducted validation under typical UWCs and HSCs. Compared with the hierarchical power management system for a fuel cell/battery hybrid electric scooter proposed by Chen, S.Y. et al., which mainly relies on a layered structure to coordinate energy distribution between the fuel cell and the battery, their method still depended heavily on manually tuned fuzzy controller parameters under complex operating conditions. In contrast, the proposed method employed WOA-GWO to automatically configure the membership functions and rule base of the fuzzy controller, thereby reducing reliance on manual adjustments. Experimental results demonstrated more stable current fluctuation control and a higher contribution rate of the SC (27.4% under UWC and 29.7% under HSC), while maintaining system efficiency at 92.6% and 94.8%, respectively.

In addition, the work of Diab et al. (2022) focused on applying the GWO and its variants for parameter estimation of PEMFCs. Their approach achieved accurate and stable parameter identification but was limited to single-source systems. In contrast, this study integrated WOA with GWO within a multi-source energy management framework. This combination improved global search capability and convergence speed while demonstrating stronger robustness in multi-energy interaction scenarios. Simulation results showed that in UWC, battery loss was reduced to 7.6% and total energy consumption to 18.3 kWh. In HSC, battery loss further decreased to 5.2% and total energy consumption to 15.4 kWh. These findings confirmed the effectiveness of the hybrid optimization strategy in improving both EE and the service life of energy storage units under diverse driving conditions.

In summary, by combining improved FC with a hierarchical game-based optimization strategy, this study proposed an automated and robust energy management approach for EVs. This method provides new insights and technological means for improving vehicle efficiency and extending storage unit life and lays a theoretical and practical foundation for intelligent power management and control in future advanced automotive systems.

5. Conclusion

To improve the efficiency and stability of EV EMSs, this study introduces a hierarchical game-based energy management method that integrates enhanced FC with a WOA-GWO hybrid optimization algorithm. The method enables automated tuning of fuzzy controller parameters and cooperative allocation between batteries and SCs. Experimental analysis confirms its effectiveness in improving overall energy utilization and stabilizing the operation of energy storage units. The proposed hierarchical game-theoretic optimization strategy enriches the theoretical perspective on integrating competition and cooperation in energy management, and demonstrates promising application potential, providing new technical pathways and methodological support for intelligent EV energy management.

Nevertheless, this study has certain limitations. The adaptability of the proposed method under extreme environmental conditions has not been fully examined, and potential communication delays and real-time computational constraints in complex road environments are not comprehensively addressed. Future research will extend validation to broader scenarios, incorporate state-of-health indicators of energy storage units, and explore adaptive mechanisms to further improve the generalizability and engineering applicability of the proposed framework.

Author Contributions

Yihui Wu contributes to conceptualization, methodology, software, validation, analysis, investigation, data collection, draft preparation, manuscript editing, and visualization. Xueqin Ran contributes to conceptualization, methodology, software, validation, analysis, draft preparation, and visualization. All authors have read and agreed with the manuscript before its submission and publication.

Funding

The research is supported by: University-level Key Scientific Research Project of Wuhu Institute of Technology. “A Multi-Source Data-Driven Study on the Mechanism of Bicycle Parking Behavior and Demand Forecasting in the Central Area of Wuhu City”. (NO, wzyzrzd202109).

Institutional Review Board Statement

Not applicable.

Declaration of AI Tools

The authors used Artificial Intelligence (AI) tools solely for language editing and readability improvement. The authors reviewed and verified all content and take full responsibility for the accuracy and integrity of the manuscript.

References

Bounemeur, A. and Chemachema, M. (2025). Finite-time output-feedback fault tolerant adaptive fuzzy control framework for a class of MIMO saturated nonlinear systems. *International Journal of Systems Science*, 56(4), 733-752.

Chen, S. Y., Lin, F. J., and Pu, T. A. (2023). Hierarchical power management system for a fuel cell/battery hybrid electric scooter. *IEEE Transactions on Transportation Electrification*, 10(2), 4583-4593.

Chu, H., Shi, H., Jiang, Y., and Shen, T. (2023). Modeling of engine thermal dynamics and its application in energy management of HEVs considering engine warming-up. *International Journal of Engine Research*, 24(1), 147-160.

Cui, N., Cui, W., and Shi, Y. (2023). Deep reinforcement learning based PHEV energy management with co-recognition for traffic condition and driving style. *IEEE transactions on intelligent vehicles*, 8(4), 3026-3039.

Diab, A. A. Z., Abdul-Ghaffar, H. I., Ahmed, A. A., and Ramadan, H. A. (2022). An effective model parameter estimation of PEMFCs using GWO algorithm and its variants. *IET Renewable Power Generation*, 16(7), 1380-1400.

Hussien, A. G., Heidari, A. A., Ye, X., Liang, G., Chen, H., and Pan, Z. (2023). Boosting whale optimization with evolution strategy and Gaussian random walks: An image segmentation method. *Engineering with Computers*, 39(3), 1935-1979.

Kuterbekov, K. A., Bekmyrza, K. Z., Kabyshev, A. M., Kubenova, M. M., and Shokatian-Beiragh, M. (2024). Fuzzy controller system utilization to increase the hydrogen production bioreactor capacity: toward sustainability and low carbon technology. *International Journal of Low-Carbon Technologies*, 19, 667-675.

Long, X. M., Chen, Y. J., and Zhou, J. (2023). Development of AR experiment on electric-thermal effect by open framework with simulation-based asset and user-defined input. *Artificial Intelligence and Applications*, 1(1), 52-57.

Mehraban, A., Farjah, E., Ghanbari, T., and Garbuio, L. (2023). Integrated optimal energy management and sizing of hybrid

battery/flywheel energy storage for electric vehicles. *IEEE Transactions on Industrial Informatics*, 19(11), 10967-10976.

Modu, B., Abdullah, M. P., Bukar, A. L., and Hamza, M. F. (2023). A systematic review of hybrid renewable energy systems with hydrogen storage: Sizing, optimization, and energy management strategy. *International Journal of Hydrogen Energy*, 48(97), 38354-38373.

Poonam, Pareek, K., and Jangid, D. K. (2022). Analysis of the effect of different factors on the degradation of supercapacitors. *Ionics*, 28(10), 4527-4545.

Precup, R. E., Nguyen, A. T., and Blažič, S. (2024). A survey on fuzzy control for mechatronics applications. *International Journal of Systems Science*, 55(4), 771-813.

Rezaie, F., Panahi, M., Bateni, S. M., Jun, C., Neale, C. M., and Lee, S. (2022). Novel hybrid models by coupling support vector regression (SVR) with meta-heuristic algorithms (WOA and GWO) for flood susceptibility mapping. *Natural Hazards*, 114(2), 1247-1283.

Shen, Y., Xie, J., He, T., Yao, L., and Xiao, Y. (2023). CEEMD-fuzzy control energy management of hybrid energy storage systems in electric vehicles. *IEEE Transactions on Energy Conversion*, 39(1), 555-566.

Simon, K., Vicent, M., Addah, K., Bamutura, D., Atwiine, B., Nanjeb, D., and Mukama, A. O. (2023). Comparison of deep learning techniques in detection of sickle cell disease. *Artificial Intelligence and Applications,* 1(4), 252-259.

Sun, B., Xie, M., Li, B., Wang, P., and Gao, S. (2024). Design and application of flywheel–lithium battery composite energy system for electric vehicles. *International Journal of Automotive Technology*, 25(1), 107-117.

Sun, P., Song, X., Song, S., and Stojanovic, V. (2023). Composite adaptive finite-time fuzzy control for switched nonlinear systems with preassigned performance. *International Journal of Adaptive Control and Signal Processing*, 37(3), 771-789.

Tan, X., Chen, Y., Zeng, J., Liao, W., and Liu, J. (2024). An integrated self-modularized battery equalizer and supercapacitor charger for hybrid electric vehicle energy storage system. *IEEE Transactions on Vehicular Technology*, 73(7), 9865-9877.

Zhang, Y., Qiu, Y., Armaghani, D. J., Monjezi, M., and Zhou, J. (2024). Enhancing rock fragmentation prediction in mining operations: A Hybrid GWO-RF model with SHAP interpretability. *Journal of Central South University*, 31(8), 2916-2929.

Zhao, S., Zhou, L., Zhang, Q., Dang, S., Yu, H., Zhang, G., Guo, R., and Zhao, W. (2022). Research on electric vehicle-supercapacitor hybrid system participates in the application of tracking PV project output. *Energy Science and Engineering*, 10(1), 120-131.

Yihui Wu obtained a bachelor's degree in Transportation from Nanjing Forestry University in 2009. Presently, he is a lecturer at the School of Automotive and Aviation at Wuhu Vocational Technical University. He has presided over multiple teaching and research projects. He has published articles in domestic academic journals. His research interests include intelligent vehicles, new energy vehicles, and by-wire chassis.

Xueqin Ran earned a master's degree in Materials Engineering from South China University of Technology in 2022. Presently, she is a lecturer at the School of Automotive and Aviation at Wuhu Vocational Technical University. She has published articles in domestic academic journals. Participate in the research of the National Natural Science Foundation of China project. Her research interests include intelligent vehicles, new energy vehicles, and by-wire chassis.